*Physiol Genomics* 50: 770–779, 2018.
First published June 29, 2018; doi:10.1152/physiolgenomics.00051.2018.

**RESEARCH ARTICLE** | *Physiological Genomics of Cell States and Their Regulation and Single Cell Genomics*

# Influenza virus infection modulates the death receptor pathway during early stages of infection in human bronchial epithelial cells

**Sreekumar Othumpangat, Donald H. Beezhold, and John D. Noti**

*Allergy and Clinical Immunology Branch, Health Effects Laboratory Division, National Institute for Occupational Safety and Health, Centers for Disease Control and Prevention, Morgantown, West Virginia*

Submitted 18 April 2018; accepted in final form 28 June 2018

**Othumpangat S, Beezhold DH, Noti JD.** Influenza virus infection modulates the death receptor pathway during early stages of infection in human bronchial epithelial cells. *Physiol Genomics* 50: 770–779, 2018. First published June 29, 2018; doi:10.1152/physiolgenomics.00051.2018.—Host-viral interaction occurring throughout the infection process between the influenza A virus (IAV) and bronchial cells determines the success of infection. Our previous studies showed that the apoptotic pathway triggered by the host cells was repressed by IAV facilitating prolonged survival of infected cells. A detailed understanding on the role of IAV in altering the cell death pathway during early-stage infection of human bronchial epithelial cells (HBEpCs) is still unclear. We investigated the gene expression profiles of IAV-infected vs. mock-infected cells at the early stage of infection with a PCR array for death receptor (DR) pathway. At early stages infection (2 h) with IAV significantly upregulated DR pathway genes in HBEpCs, whereas 6 h exposure to IAV resulted in downregulation of the same genes. IAV replication in HBEpCs decreased the levels of DR pathway genes including TNF-receptor superfamily 1, Fas-associated death domain, caspase-8, and caspase-3 by 6 h, resulting in increased survival of cells. The apoptotic cell population decreased in 6 h compared with the 2 h exposure to IAV. The PCR array data were imported into Ingenuity Pathway Analysis software, resulting in confirmation of the model showing significant modulation of the DR pathway. Our data indicate that a significant transcriptional regulation of apoptotic, necrotic, and DR genes occur at early and late hours of infection that are vital in modulating the survival of host cells and replication of IAV. These data may have provided a likely roadmap for translational approaches targeting the DR pathway to enhance apoptosis and inhibit replication of the virus.

caspase-8; Death receptor, FADD, influenza virus, lung epithelial cells

## INTRODUCTION

Influenza A viruses (IAV) belong to the Orthomyxoviridae family of human respiratory pathogens that cause periodic pandemics (18, 32). In the United States, the annual direct costs of influenza are estimated at $4.6 billion along with up to 111 million lost workdays (5, 6). Vaccination is still considered as the best method of prevention of this disease but has limitations as the virus periodically undergoes antigenic shift and drift, rendering the vaccine less effective (1). Understanding the molecular mechanism of IAV infection and damage to the epithelial cells of the respiratory tract could lead to novel methods of prevention. Several studies suggest that apoptosis is one mechanism epithelial cells use to halt viral replication (18), but the mechanism or pathways targeted in early stages of IAV infection has not been studied in detail. To expand our understanding on the survival of virus in host cells, the apoptotic, necrotic, and death receptor (DR) pathways were investigated.

Apoptosis is a fundamental biochemical process of selective and controlled elimination of infected or damaged cells as a defense mechanism against invading pathogens (28, 37). Apoptosis also plays an important role in the pathogenesis of many infectious diseases (11, 21, 29). Earlier studies reported the occurrence of apoptotic-triggering events in virus-infected cells (30, 38). IAV also induces apoptotic cell death in infected epithelial and lymphocyte cells (33, 34). IAV replication in lung cells showed cytopathic effect followed by cell death (31). Programmed cell death occurs in cells through either intrinsic or extrinsic apoptotic pathways. The intrinsic pathway is triggered by changes in mitochondrial integrity and involves the release of cytochrome c into the cytosol and the activation of caspase-9 (10). The extrinsic pathway is initiated through the death receptors FasR and tumor necrosis factor receptor (TNFR) and involves the activation of caspase-8 (9). Two important pathways activate caspase cascades for apoptosis, the DR pathway, and the mitochondrial signaling pathway (13).

The TNFR superfamily plays a central role in the physiological regulation of programmed cell death and is implicated in the pathogenesis of various diseases of the immune system (2). Tumor necrosis factor-α (TNF-α), a pleiotropic cytokine, functions by binding to the receptors designated as TNFR1 and TNFR2 (38). Among the DRs, the type 1 transmembrane protein receptors have a conserved cytoplasmic motif found on all of the three receptors (FasR, TNFR1, and TNFR2), and on TNF-related apoptosis-inducing ligand receptor 1 and 2 (TRAILR1 and TRAILR2; also known as DR4 and DR5, respectively) that binds with Fas-associated death domain (FADD) activating caspase-8. DR4 and DR5 require death-associated protein 3 (DAP3) for recruitment of FADD (22). FADD thus plays a pivotal role in DR-mediated apoptosis. Activated caspase-8 transmits the apoptotic signal either by directly cleaving and activating downstream

Address for reprint requests and other correspondence: S. Othumpangat, Allergy and Clinical Immunology Branch, 1095 Willowdale Rd., MS 4020, National Institute for Occupational Safety and Health, Morgantown, WV 26505 (e-mail: seo8@cdc.gov).

caspases or by cleaving the BH3-Bcl2-interacting protein that releases cytochrome c from mitochondria initiating the activation of caspase-9 (18).

TNFR1 signaling differs from FasR or TRAILR1/TRAILR2-induced apoptosis. Fas receptor contains a death domain directly interacting with FADD (7), whereas TNFR1 requires TNFR type 1-associated death domain protein (TRADD) to recruit FADD. Two sequential signaling complexes are involved in TNFR1-induced apoptosis. Plasma membrane bound complex (complex-I) consists of TNFR1, TRADD, receptor-interacting protein (RIP), TNFR-associated factor 2 (TRAF2), which functions to activate NF-kappa B (NF-κB). In a second step, TRADD and RIP associate with FADD and caspase-8, forming a cytoplasmic complex-II. When NF-κB is activated by complex-I, complex-II associates with caspase-8 and activates inhibitor protein FLIP, leading to the survival of the host cell.

IAV relies on host genes for its replication and survival (17) and modulates the signaling pathways of the host cells to promote viral replication (20, 21, 36). IAV infection induces the upregulation of several proapoptotic factors, while inhibition of TRAIL and FAS results in increased viral copy numbers (35). To understand the DR cascade in detail, we first investigated the DR pathway gene profiles of IAV infected human bronchial epithelial cells (HBEpCs) to mock-infected cells. We demonstrate that induction of the DR pathway is one mechanism by which host cells eliminate IAV-infected cells. To characterize the functional consequences of gene expression changes associated with infection by IAV, we performed pathway analysis of our gene expression data using Ingenuity Pathways Analysis (IPA). IPA results showed that initial infection with IAV induced the DR pathway in infected HBEpCs at 2 h postinfection and activates FADD-mediated caspases through the mitochondrial pathway. By 6 h postinfection, IAV overcomes the downregulation of DR pathway genes and reduces the number of apoptotic cells while increasing viral copy numbers in epithelial cells.

## METHODS

*Cell culture.* Primary HBEpCs were purchased from Promo Cells (Hamburg, Germany) and cultured as instructed by the manufacturer in bronchial epithelial cell growth media. Madin-Darby canine kidney (MDCK) cells were used to propagate IAV, as described in earlier studies (24). MDCK cells were cultivated in MEM medium supplemented with 10% FBS and 100 IU/ml penicillin and 100 μg/ml streptomycin sulfate. Influenza strain A/WSN/33 was a kind gift from Prof. Robert Lamb (Northwestern University) and A/Aichi/2/68 (H3N2-ATCC 1680) was procured from ATCC and maintained as described earlier (25).

*Viral infections.* All infections of HBEpC were done in six-well plates at a dose of 1.0 multiplicity of infection (MOI) unless otherwise specified. Six-well plates were seeded with $5 \times 10^5$ cells per well and grown to 80% confluence. Prior to infection, the cells were washed with PBS, and the virus was diluted in modified Hans balanced saline solution and added to each well. After 45 min of incubation at 37°C and 5% $CO_2$, the unbound viruses were washed off with 2 ml PBS. For H3N2, fresh F12 media containing 0.5 μg/ml of TPCK-trypsin (Sigma-Aldrich, St. Louis, MO) was added, and for H1N1 (WSN), F12 medium without TPCK was added to the cells and incubated at 37°C and 5% $CO_2$. Cells were then harvested at various time intervals and used for RNA and protein studies.

*SuperArray analysis.* Predesigned PCR array plates purchased from SuperArray Technology (catalogue no. PAHS-141Z; SABiosciences, Frederick, MD) and were utilized to compare the relative levels of mRNA from apoptosis-related genes expressed in HBEpCs infected with IAV for 2 h and 6 h at MOI of 1.0. The array plate contained 84 primer pairs that amplified genes involved in human necrosis pathway including the DR pathway genes. The infected and the mock-infected cells were analyzed in three independent experiments with $RT^2$ SYBR green ROX qPCR master mix. The RT-PCR reaction was analyzed on an ABI 7500 instrument (Applied Biosystems, Foster City, CA). The mean value for each gene was determined and used to calculate the fold changes in expression (infected vs. mock-infected control) using QIAGEN's online array analysis software.

*RNA isolation.* RNA was isolated from HBEpCs using the RNeasy plus kit (Qiagen, Valencia, CA) according to the manufacturer's instructions, and 1.0 μg RNA was used to generate cDNA with the High capacity ABI-RT PCR kit (Applied Biosystems). RT-PCR reactions were done using the TaqMan FAST PCR reagent (Applied Biosystems) and the ABI 7500 FAST real-time cycler (Applied Biosystems). TaqMan primers for FADD, TNFRSF1, Caspase-3, Caspase-8, and glyceraldehyde phosphate dehydrogenase (GAPDH) were purchased from Thermo Fisher Scientific (Thermo Fisher Scientific, Waltham, MA). Influenza matrix gene expression was quantified with a standard curve and reported as copy numbers of IAV. Gene expression was normalized to GAPDH and reported as fold change. The change in gene expression was calculated thus: fold change = 2^(ddCt), ddCt is the dCt (H1N1-infected) − dCt (mock-infected), where dCt = Ct (detected gene) − Ct (GAPDH) and Ct is the threshold number.

*Western blot analysis.* At specific time points after influenza virus infection and as indicated in the figure legends, infected cells were lysed in radioimmunoprecipitation assay (RIPA) buffer (Thermo-Fisher Scientific) containing a complete protease inhibitor cocktail. Isolated protein was used for Western blot analysis using a 10% SDS-polyacrylamide gels (SDS-PAGE, Pre-cast gels, Bio-Rad) and PVDF membrane. Membranes were probed with anti-rabbit polyclonal antibodies to FADD, DR3, DR5 (dilution 1:200; Cell Signaling, Danvers, MA), and anti-mouse monoclonal anti-GAPDH (dilution 1:10,000; Abcam, Cambridge, MA). Near-infrared fluorescence detection was performed on the Odyssey Imaging System (LI-COR Biosciences), and the fluorescent signal intensities of the individual bands were determined.

*Imaging with confocal microscopy.* HBEpCs were grown on chamber slides (Chamber slide, Lab-TekII; Thermo Fisher Scientific, Rochester, NY) and infected with H1N1 or H3N2 for 2–6 h. Confocal staining of the cells was done as described earlier (25). Cells were treated with rabbit anti-human FADD or DR3 antibody (Cell Signaling) and anti-mouse TRADD (Millipore, Billerica, MA) followed by a secondary Alexa-488 conjugated anti-rabbit antibody and Alexa-546 conjugated anti-mouse antibody (Invitrogen).

*Flow cytometric analysis for apoptotic cells.* HBEpCs ($1 \times 10^6$) were infected with H1N1 and H3N2 at MOI of 1 for 2–6 h. Cells were harvested, resuspended in 100 μl of annexin 1× binding buffer, and stained for 15 min at room temperature with 5 μl of annexin V-FITC (BD Biosciences) and 5 μl of propidium iodide (BD Biosciences) to detect apoptosis and necrosis, respectively. After the addition of 300 μl of 1× binding buffer to each sample, flow cytometry analysis was performed with FACS LSRII (BD Biosciences). Data were collected with CellQuest software (BD Biosciences).

*IPA.* The mRNA fold changes from the PCR array data obtained from the Qiagen online data analysis software were imported directly into the IPA software (Qiagen, Redwood City, CA) for core analysis and pathway generation. IPA-generated networks show differentially regulated genes that may be related according to previously validated studies between genes or proteins, described in the literature. The data from 2 and 6 h exposure of both (H1N1 and H3N2) strains of IAV were used to generate potential interactions among the pathway genes

in the DR pathway. The Core Analysis function included in IPA interprets the data in the context of biological processes, pathways, and networks (16). Both up- and downregulated genes were defined as value parameters for the analysis. IPA-generated networks are ordered by a score meaning significance. Canonical pathways were grouped into metabolic pathways and signaling pathways.

*Statistical analysis.* One-way analysis of variance (ANOVA) was used to analyze the PCR data, and post hoc pairwise multiple comparisons between means were performed as per the Holm-Sidak method with Sigma Stat version 11.0 for Windows (Systat Software, Chicago, IL). A $P$ value of $<0.05$ was considered statistically significant.

## RESULTS

*PCR array for necrosis and apoptosis.* Previous studies from our laboratory have indicated that early stage infection (1–3 h) leads to the induction of apoptotic protein caspase-9 (25). These data also suggest that the initial cellular defense would try to eliminate infected cells by driving them into the apoptotic state. Takizawa et al. (31) have suggested that influenza infection causes apoptotic death of cultured cells at an early stage of infection by the induction of the FAS gene. Moreover, examining the initial stages of infection addresses the primary response of host cells against the invading viruses. To further understand the apoptotic pathway involved in early and late stages of IAV infection, we first assessed the effect of IAV infection at 2 and 6 h on necrosis and apoptosis genes in HBEpCs with PCR array analysis. HBEpCs were infected with either H1N1 or H3N2 at an MOI of 1.0 for 2 and 6 h, and 84 key genes involved in programmed necrosis, death receptor signaling, ROS production, and mitochondrial activity were evaluated with Human Necrosis RT$^2$ Profiler PCR Super Array (Table 1). Genes that are central to apoptosis (Table 1*C*) and necrosis (Table 1*B*) showed a significant difference in gene expression at both 2 and 6 h postinfection. By 2 h, most of the DR signaling pathway genes (Table 1*A*), including FADD (1.5- to 1.7-fold), FAS (1.63- to 1.88-fold), DR3 (3.1- to 4.6-fold), and TRADD (1.54- to 1.69-fold) showed significant increases in expression compared with mock-infected cells. FADD, considered as the common mediator of apoptosis by death domain receptors (DR3, and DR4) increased 1.7- and 1.5-fold at 2 h postinfection with H1N1 and H3N2, respectively. By 6 h, FADD (2.1- and 2-fold), Fas (1.2- and 1-fold), and TRADD (1.0- and 1.2-fold) was downregulated in HBEpCs infected with H1N1 and H3N2, respectively.

*DR pathway.* Data obtained from the PCR array were further clarified by quantifying the fold changes in DR pathway genes with RT-PCR in a time course study (1–6 h). HBEpCs exposed to H1N1 at an MOI of 1.0 and the gene expression levels of TNFRSF1, FADD, caspase-8, and caspase-3 from RT-PCR are shown in Fig. 1. At 1 h postinfection, TNFRSF1 and FADD expression increased 1.7- and 2.4-fold, respectively, and remained elevated at 2 h postinfection and then gradually decreased to levels nearly twofold lower than that of uninfected cells by 6 h. Expression of Caspase-8 increased 1.6-fold 1 h postinfection and then gradually decreased to 0.45-fold lower than that of uninfected cells by 6 h. Caspase-3 showed a small (1.2-fold) increase in expression at 1 h postinfection and also gradually decreased to 0.6-fold lower than that of uninfected cells by 6 h postinfection. Our findings suggest that the IAV-infected cells tend to transition from an apoptotic state to an antiapoptotic state beginning from 2 to 6 h exposure to IAV. This statement is supported by the data presented in Fig. 4, which suggest that this is very likely in the majority of the cells and not necessarily with all the cells exposed to IAV.

To determine whether the transcriptional changes in RNA levels of these genes were accompanied by translational changes, protein expression was examined by Western blot analysis. HBEpCs were infected with either H1N1 or H3N2 at an MOI of 1.0 for 6 h, and protein expression was assessed 2 and 6 h postinfection. FADD expression was significantly increased 1.8- and 1.9-fold at 2 h postinfection with both strains, but by 6 h, expression in H1N1-infected cells was reduced to lower (0.8-fold) than that of the uninfected cells (mock) and similarly reduced (0.2-fold) in H3N2-infected cells (Fig. 2, *A* and *C*). Other major proteins of the DR pathway, DR3 and DR5 were also 1.8- to 2.6-fold elevated at 2 h postinfection but returned to levels lower (0.4- to 0.7-fold) (Fig. 2, *B* and *C*) than uninfected cells by 6 h with both strains of IAV. Taken together, these results further suggest that DR pathway proteins may play a significant role in viral survival at 2–6 h of infection.

The increased expression of FADD and DR3 in infected cells shown by Western blot was also confirmed by confocal microscopy along with expression of TRADD. Expression of all three proteins was dependent on the exposure time to H1N1. FADD and TRADD expression increased at 2 h postinfection and returned to those levels in uninfected cells or lower by 6 h (Fig. 3*A*) Similarly, DR3 expression increased at 2 h and declined to that in uninfected cells by 6 h (Fig. 3*B*). Similar results were obtained with H3N2 (data not shown).

We also analyzed annexin V staining (apoptosis) and PI uptake (necrosis) to compare the apoptotic and necrotic state of IAV-infected cells. Figure 4*A* shows that the early-stage infection (2 h exposure) of bronchial epithelial cells resulted in a decrease in the viable cells and increase in apoptotic and necrotic cells with both H1N1 and H3N2 strains of IAV. Consequently, the increase in exposure time (6 h) increased the total viable cells and decreased the number of apoptotic and necrotic cell population. The decrease in these two cell populations at 6 h of exposure to IAV could be due to the change in DR pathway signaling.

Meanwhile, we also measured whether the viral population increased with increase in exposure time, to ascertain that virus are alive and active, irrespective of the modulation of DR pathway. The viral copy numbers are expressed as IAV matrix gene copy numbers in HBEpCs infected with either H1N1 or H3N2 (Fig. 4*B*). We did not see any significant morphological changes in cell phenotype, from 2 to 6 h exposure to IAV, although few cells showed increase in cell size. In addition, a 2–6 h exposure to IAV resulting in a 10-fold increase in viral copy numbers suggests that the viruses are active and multiplying in HBEpCs.

*Pathway analysis.* The data obtained from the PCR array (Table 1) were subjected to IPA, which subsequently revealed multiple pathways that appear to be the targets of IAV infection. The resulting changes to expression of DR pathway proteins 2 h postinfection of H1N1 in HBEpCs are shown (Fig. 5). The DR pathway shows the interaction between FAS and FADD that results in the induction of the caspase pathway for apoptosis through mitochondrial release of cytochrome c. The increased levels of FAS induced the expression of FADD,

Table 1. *PCR array data showing the differential expression of necrotic and apoptotic, including Death Receptor pathway genes on exposure to influenza virus for 2 and 6 h*

| Gene Symbol | H1N1 2 h | H1N1 6 h | H3N2 2 h | H3N2 6 h |
|---|---|---|---|---|
| *A. Death receptor signaling genes* | | | | |
| BID | 1.6705 | −1.1268 | 1.2614 | −1.0866 |
| BIRC3 | −8.4445 | −7.2751 | −11.4404 | −11.091 |
| CASP8AP2 | −1.3401 | 1.0153 | −1.0121 | 1.1755 |
| CYLD | 2.2992 | 2.7979 | 1.989 | 3.0698 |
| EDA2R | −3.4018 | −6.9352 | −7.3251 | −2.097 |
| FADD | 1.7047 | −2.1807 | 1.4905 | −1.978 |
| FAF1 | 1.0614 | −1.2741 | 1.4664 | −1.3019 |
| FAS | 1.8874 | −1.2151 | 1.6392 | −1.026 |
| FEM1B | 1.2352 | 1.2553 | 1.2369 | 1.7072 |
| IKBKG | −1.6156 | −1.9047 | −2.039 | −1.6056 |
| MADD | −1.3741 | −1.4662 | −1.36 | −1.1086 |
| MYD88 | −1.203 | 1.0832 | −1.1268 | 1.1084 |
| NGF | 1.281 | −1.2372 | 2.0946 | −1.3989 |
| NGFR | 5.4884 | 3.4322 | 2.6526 | 2.4447 |
| NGFRAP1 | −1.5617 | −1.2735 | −1.7528 | −1.5964 |
| PARP1 | −2.3284 | −3.2725 | −2.9497 | −2.3855 |
| PIDD | −1.075 | −1.4353 | −1.7287 | −2.0342 |
| RIPK1 | 1.9498 | 1.623 | 2.3367 | 1.6484 |
| TNFRSF14 | 6.6447 | 8.0388 | 2.9152 | 2.6605 |
| TNFRSF17 | 1.8864 | −1.3944 | 1.5572 | 2.3833 |
| TNFRSF1A | 1.9153 | −2.1502 | 1.9012 | −1.7832 |
| TNFRSF1B | 2.1665 | 1.3784 | 1.6021 | −1.0989 |
| TNFRSF25 | 7.7311 | 6.5293 | 4.5171 | 3.5202 |
| TNFRSF4 | 1.0226 | 1.3128 | −2.2767 | −1.8535 |
| TNFRSF8 | −1.5617 | −1.3212 | −1.9125 | −1.5549 |
| TNFSF15 | −1.5434 | −2.8836 | −4.2282 | −3.0497 |
| TRADD | 1.5491 | −1.0779 | 1.6943 | −1.1711 |
| TRAF2 | 1.6301 | −1.9998 | 1.2761 | −1.1356 |
| *B. Necrosis genes* | | | | |
| ATP6V1G2 | −3.5123 | −3.9169 | −5.4752 | −3.9901 |
| BMF | −6.4512 | −8.1435 | −6.81 | −10.5748 |
| BNIP3L | −1.1857 | 1.0262 | −1.242 | 1.0426 |
| C1orf159 | 1.0804 | 1.065 | −1.14 | −1.0843 |
| CAPN1 | 1.2662 | 1.1387 | 1.0265 | −1.051 |
| CAPN2 | −1.0408 | 1.3585 | 1.1328 | 1.2318 |
| CAPN3 | 3.6163 | 2.479 | 2.0707 | 1.8057 |
| CAPN5 | −7.6877 | −9.6087 | −11.4503 | −10.8556 |
| CAPN6 | −1.1657 | −1.9724 | −1.5834 | −1.0764 |
| CAPN7 | 1.0424 | 1.0305 | −1.0619 | 1.1758 |
| CAPNS1 | −2.257 | −2.2775 | −3.1163 | −2.742 |
| CCDC103 | −3.931 | −3.8967 | −4.4078 | −2.6342 |
| CD40 | −2.106 | −2.8755 | −3.2768 | −3.2207 |
| COMMD4 | −1.6632 | −1.7966 | −2.1664 | −1.715 |
| CYLD | 2.2992 | 2.7979 | 1.989 | 3.0698 |
| DEFB1 | 7.6759 | 3.0889 | 10.3664 | 4.3761 |
| DENND4A | −2.0343 | −2.4644 | −2.8739 | −2.0444 |
| DPYSL4 | −1.3629 | −1.7428 | −1.6402 | −1.1259 |
| EIF5B | −1.252 | −1.155 | 1.0783 | 1.3125 |
| FADD | 1.7047 | −2.1807 | 1.4905 | −1.978 |
| FAS | 1.8874 | −1.2151 | 1.6392 | −1.026 |
| FASLG | 2.1945 | −1.6264 | 1.5099 | 1.0745 |
| FOXI1 | −1.7108 | −1.6823 | −1.8187 | −2.494 |
| FUS | −1.4395 | −1.3692 | −1.5476 | −1.0576 |
| GALNT5 | 1.8203 | 3.8357 | 3.15 | 3.2674 |
| GLUD1 | −1.5845 | −1.5201 | −1.5634 | −1.4138 |
| GLUL | 1.0629 | −1.2812 | −1.2969 | 1.0041 |
| GRB2 | −1.4866 | −1.1462 | −1.3452 | −1.0598 |
| HSPBAP1 | 1.3723 | 4.0924 | 1.3112 | 1.1853 |
| JPH3 | −10.6296 | −2.1392 | −4.3368 | −4.2977 |
| KCNIP1 | −1.3348 | −1.2061 | −1.7184 | −1.788 |
| MAG | 1.0056 | −1.0498 | −1.223 | −1.3212 |
| MGEA5 | 1.0063 | 1.0816 | −1.002 | 1.2571 |
| NFKB1 | 1.427 | −1.1534 | 1.6627 | −1.0838 |
| OR10J3 | −1.1434 | −1.0331 | −1.4719 | −1.0547 |
| PARP1 | −2.3284 | −3.2725 | −2.9497 | −2.3855 |
| PARP2 | 1.0257 | 1.1432 | 1.1172 | 1.075 |
| PPIA | −1.0143 | 1.0682 | −2.0346 | −2.0178 |
| PPID | 1.2246 | 1.8725 | 1.4468 | 1.9394 |
| PVR | −1.2733 | −1.1997 | −1.1447 | 1.0056 |
| PYGL | 1.1028 | 1.1691 | 1.1455 | 1.1911 |
| RAB25 | 8.0268 | 6.1452 | 9.1723 | 8.2581 |
| RIPK1 | 1.9498 | 1.623 | 2.3367 | 1.6484 |
| RIPK2 | −1.6746 | −1.3068 | −1.5231 | −1.1141 |
| RIPK3 | 1.6576 | 1.1383 | 2.1428 | 1.616 |
| SP1 | −1.2149 | −1.0976 | −1.1709 | 1.0089 |
| SYCP2 | −2.9317 | −2.0818 | −11.1565 | −4.1291 |
| TMEM123 | −1.2096 | 1.0011 | −1.4118 | −1.167 |
| TMEM57 | 1.2176 | 1.2108 | 1.1792 | 1.6443 |
| TNF | 10.9313 | 22.5609 | 5.5303 | 6.5998 |
| TXNL4B | −1.058 | 1.176 | 1.0027 | 1.4085 |
| *C. Apoptotic genes* | | | | |
| AIFM1 | −1.7127 | −1.8578 | −1.88 | −1.6802 |
| ATP6V1G2 | −3.5123 | −3.9169 | −5.4752 | −3.9901 |
| BAX | −1.8561 | −1.7336 | −2.3757 | −2.3312 |
| BID | 1.6705 | −1.1268 | 1.2614 | −1.0866 |
| BIRC3 | −8.4445 | −7.2751 | −11.4404 | −11.091 |
| BMF | −6.4512 | −8.1435 | −6.81 | −10.5748 |
| CASP8AP2 | −1.3401 | 1.0153 | −1.0121 | 1.1755 |
| CYLD | 2.2992 | 2.7979 | 1.989 | 3.0698 |
| FADD | 1.7047 | −2.1807 | 1.4905 | −1.978 |
| FAF1 | 1.0614 | −1.2741 | 1.4664 | −1.3019 |
| FAS | 1.8874 | −1.2151 | 1.6392 | −1.026 |
| FASLG | 2.1945 | −1.6264 | 1.5099 | 1.0745 |
| FEM1B | 1.2352 | 1.2553 | 1.2369 | 1.7072 |
| IKBKG | −1.6156 | −1.9047 | −2.039 | −1.6056 |
| MADD | −1.3741 | −1.4662 | −1.36 | −1.1086 |
| MYD88 | −1.203 | 1.0832 | −1.1268 | 1.1084 |
| NFKB1 | 1.427 | −1.1534 | 1.6627 | −1.0838 |
| NGF | 1.281 | −1.2372 | 2.0946 | −1.3989 |
| NGFR | 5.4884 | 3.4322 | 2.6526 | 2.4447 |
| NGFRAP1 | −1.5617 | −1.2735 | −1.7528 | −1.5964 |
| RIPK1 | 1.9498 | 1.623 | 2.3367 | 1.6484 |
| RIPK2 | −1.6746 | −1.3068 | −1.5231 | −1.1141 |
| RIPK3 | 1.6576 | 1.1383 | 2.1428 | 1.616 |
| SPATA2 | −1.1353 | 1.0954 | −1.0413 | 1.2261 |
| SYCP2 | −2.9317 | −2.0818 | −11.1565 | −4.1291 |
| TNF | 10.9313 | 22.5609 | 5.5303 | 6.5998 |
| TNFRSF10A (TRAIL-R) | 1.5089 | −1.2016 | 1.9785 | 1.3041 |
| TNFRSF1A | 1.9153 | −2.1502 | 1.9012 | −1.7832 |
| TNFRSF1B | 2.1665 | 1.3784 | 1.6021 | −1.0989 |
| TNFRSF25 (DR3) | 7.7311 | 6.5293 | 4.5171 | 3.5202 |
| TNFRSF4 | 1.0226 | 1.3128 | −2.2767 | −1.8535 |
| TNFRSF8 | −1.5617 | −1.3212 | −1.9125 | −1.5549 |
| TNFSF10 (TRAIL) | 4.6843 | 2.123 | 3.1589 | 2.0027 |
| TRADD | 1.5491 | −1.0779 | 1.6943 | −1.1711 |
| TRAF2 | 1.6301 | −1.9998 | 1.2761 | −1.1356 |

*A*: death receptor genes; *B*: necrotic genes; *C*: apoptotic genes. Human bronchial epithelial cells were infected with H1N1 or H3N2 strains of influenza virus at multiplicity of infection of 1 for 2 or 6 h. Cells harvested and RNA isolated were used for CDNA synthesis. Diluted cDNA was used for PCR array.

which in turn activates the caspase-8 (1.6-fold increase, Fig. 2*C*) pathway (all increased expression shown in red in Fig. 5). Activated caspase-8 stimulates apoptosis by cleaving BID (1.6-fold increase, Table 1) to initiate apoptosis through the release of cytochrome C. Once Bid is cleaved by caspase-8, truncated Bid (tBid) migrates from the cytosol to the mitochondrial outer membrane, where it stimulates Bax to oligomerize

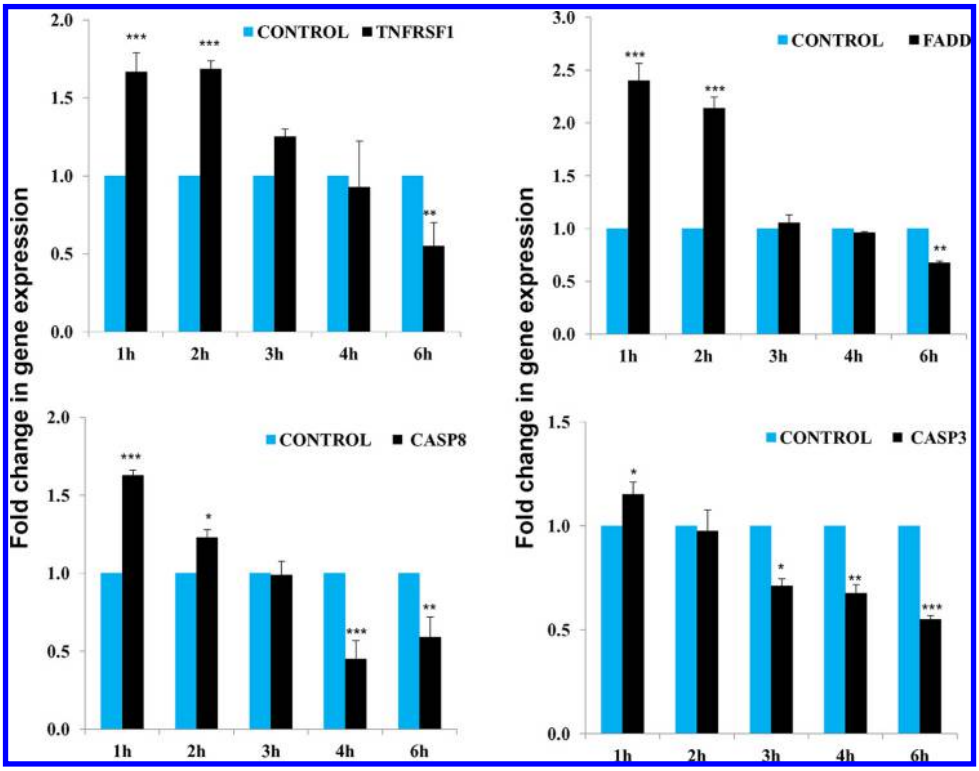


Fig. 1. Influenza A virus (IAV) infection induces expression of death receptor (DR) genes. Human bronchial epithelial cells (HBEpCs) were infected with IAV H1N1 for 1–6 h, and total RNA was extracted from the infected cells. cDNA was synthesized from 1 μg of RNA and subjected to quantitative (q)PCR analysis using specific primers ($n = 3$). Expression of DR genes was normalized to GAPDH expression by the ddCT method. ***$P < 0.001$, **$P < 0.01$, and *$P < 0.05$.

and alters the mitochondrial outer membrane, leading to the release of cytochrome c. Subsequently, this then blocks the caspase inhibitor XIAP and promotes the activation of caspase-9. Caspase-9 in turn cleaves and activates caspase-3, leading to apoptosis (8).

Caspase-3-mediated apoptosis may prevail in IAV-infected cells. Our model showed that induction of apoptosis occurs through TNF, inducing TNFRSF1A (2-fold increase at 2 h), which binds with TRADD and FADD to facilitate the downstream process of apoptosis. Induction of the DR pathway gene TNFRSF25 (DR3) by 2 h postinfection occurs following binding to its ligand and activation of TRADD/FADD. This complex can activate caspase-8/-10; initiating caspase-3-mediated apoptosis. Another mechanism that initiates caspase-3-medi-

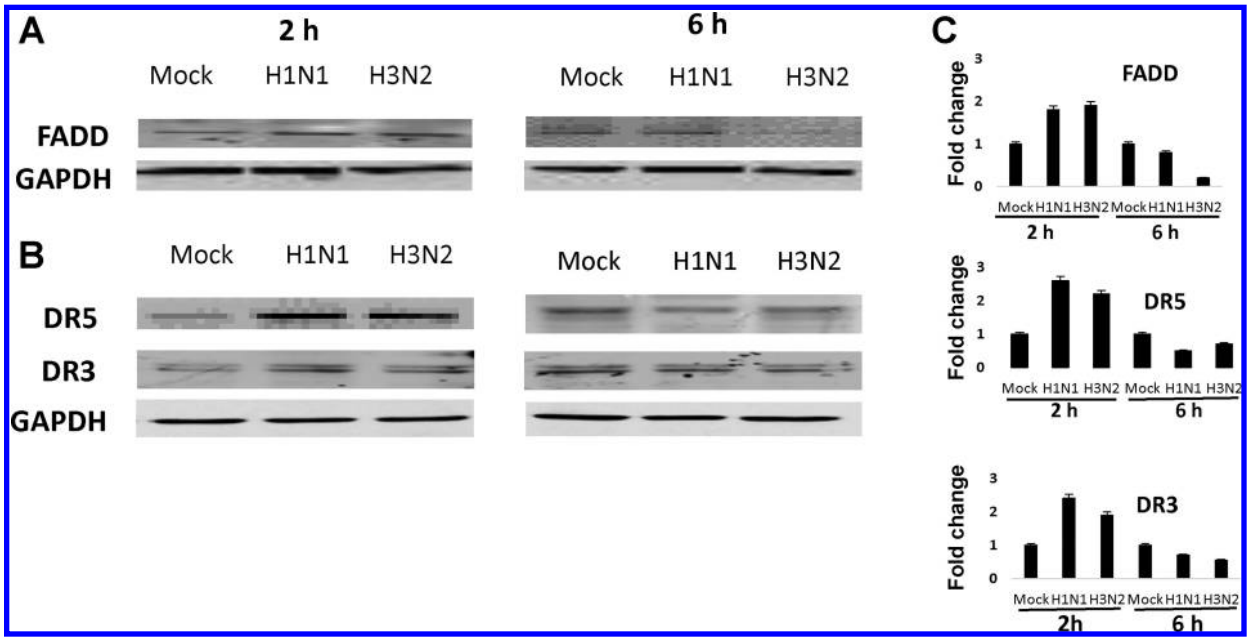


Fig. 2. Western blot analysis showing differential expression of DR pathway proteins in IAV-infected HBEpCs. *A*: Fas-associated death domain (FADD) and corresponding housekeeping protein GAPDH. *B*: DR5, DR3, corresponding housekeeping protein GAPDH. HBEpCs were grown to 80% confluence and infected with IAV H1N1 or H3N2 at multiplicity of infection (MOI) of 1 for 2 or 6 h. *C*: fold increase in expression was determined by densitometry and normalized to GAPDH.

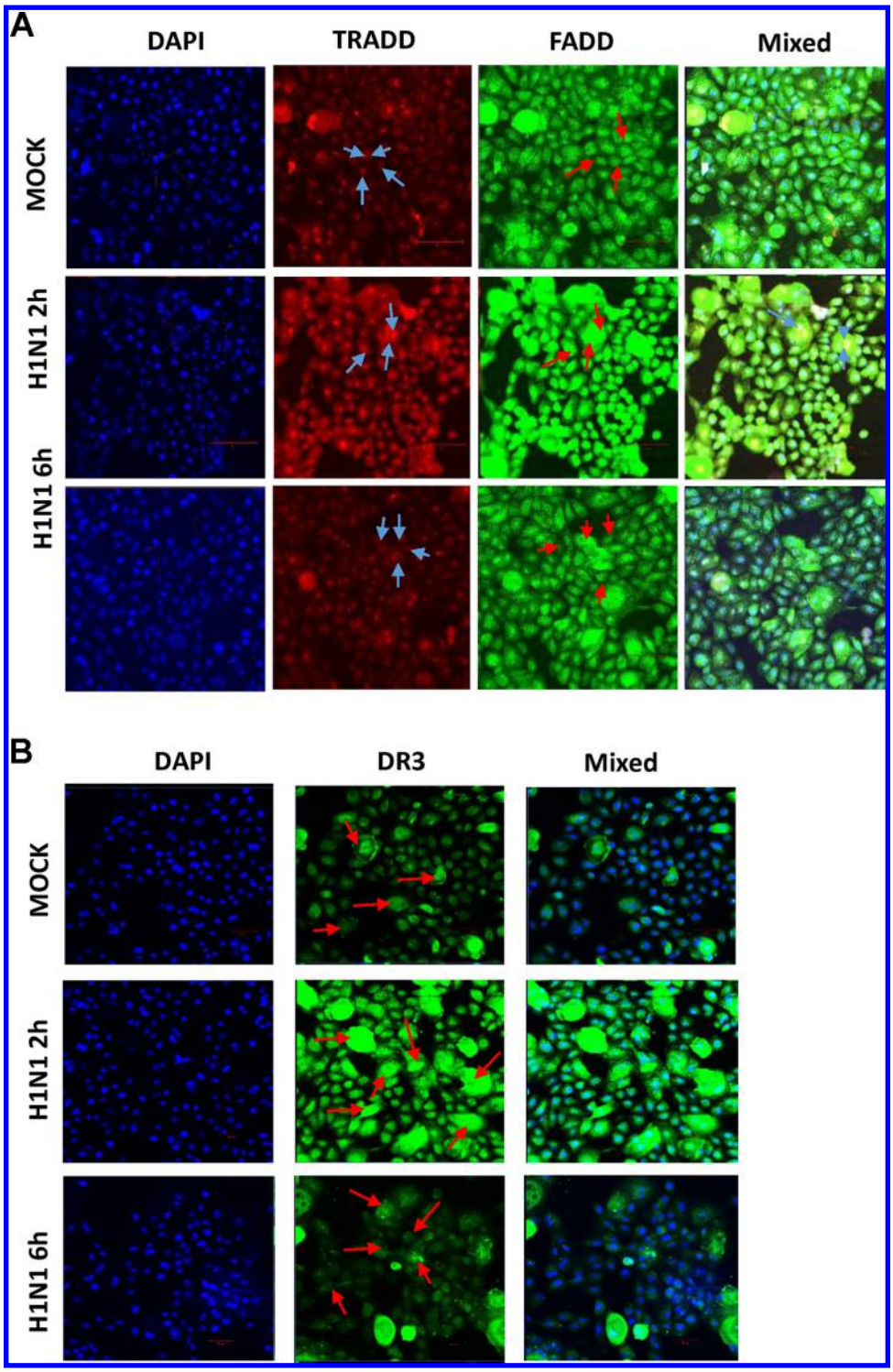


Fig. 3. Differential expression of DR pathway proteins in IAV-infected HBEpCs detected by immunofluorescence. *A*: expression of FADD and TNFR type 1-associated death domain protein (TRADD) in infected HBEpCs. Cells were stained with anti-FADD antibodies (green), anti-TRADD (red), and the nucleus by DAPI (blue) *B*: expression of DR3 in infected HBEpCs. Cells were stained with anti-DR3 antibodies (green) and the nucleus by DAPI (blue). Arrows highlight the cells showing differential expression of proteins. HBEpCs were infected with H1N1 at an MOI of 1.0 or mock-infected. After virus adsorption for 45 min at 37°C, the cells were incubated for 2 or 6 h. Thereafter, cells were washed, fixed, and processed for immunofluorescence staining. Images were obtained under a Zeiss LSM510 confocal microscope equipped with the AxioImager system (Carl Zeiss, Obertochen, Germany).

ated apoptosis through the activation of caspase-8/-10 is through the induction of TNSF10, which activates DR4/5, a complex that binds to FADD, as illustrated in the schematic representation of DR pathway (Figs. 5 and 6). Caspase-8 activates caspase-3, which could lead to apoptosis through membrane blebbing, chromatin condensation, DNA fragmentation, or cell shrinkage. We also saw a decrease in apoptotic cells in 6 h exposure compared with the 2 h exposure to IAV, confirming the PCR array data.

Interestingly, 6 h post-H1N1 infection of HBEpCs resulted in significant downregulation of most of the DR pathway genes (shown in green in the schematic figures) including FAS, FADD, and BID, that shut down the pathway leading to apoptosis (Fig. 6). In addition, decreased FADD expression resulted in reduced interaction between the DR4/5 proteins, inhibiting the DR pathway. Moreover, IAV-induced expression of mRNAs of FADD, Caspase-8, and Caspase-3 was significant at 1–2 h postinfection (Figs. 1–3), prompting the cells into

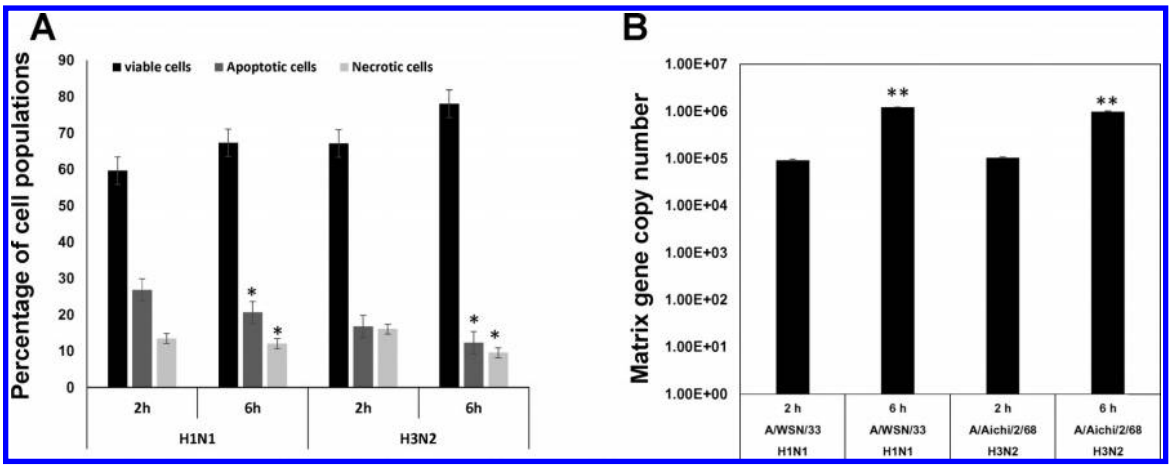


Fig. 4. Change in influenza matrix gene copy numbers and cell population of HBEpCs infected with IAV. *A*: HBEpCs were infected with 1 MOI of influenza A H1N1 or H3N2 for 2–6 h. The cells were fluorescently labeled with annexin V and PI, and the different cell populations were analyzed by flow cytometry. Data are expressed as ± SE; $*P < 0.05$ compared with 2 and 6 h of infection ($n = 3$). *B*: matrix copy number in cells infected with either H1N1 or H3N2. HBEpCs were grown to 80% confluence and infected with IAV H1N1 or H3N2 at MOI of 1 for 2 or 6 h. Data are expressed as ± SE, $**P < 0.01$ compared with 2 and 6 h of infection ($n = 3$).

apoptosis, but the decrease in expression of these transcripts following the 3–6 h postinfection reverses the apoptotic activity as these proteins have a central roles in the induction of apoptosis through the DR and mitochondrial apoptosis pathways.

## DISCUSSION

The purpose of apoptosis or programmed cell death is to maintain homeostasis in mammals and control invading pathogens (13). Our data indicated that apoptosis and caspase activation on exposure to IAV was initiated at the very early stages of infection, at least, partly through the activation of the DR pathway genes including FADD, TNFR2, DR3, and DR5 at 2 h postinfection of IAV in HBEpCs. The DR ligands initiate signaling through receptor oligomerization, which in turn recruit specialized adaptor proteins (such as FADD) to activate a cascade of caspases. Binding of Fas ligand (1.5- and 2.9-fold increase in H3N2 and H1N1, respectively; Table 1) induces

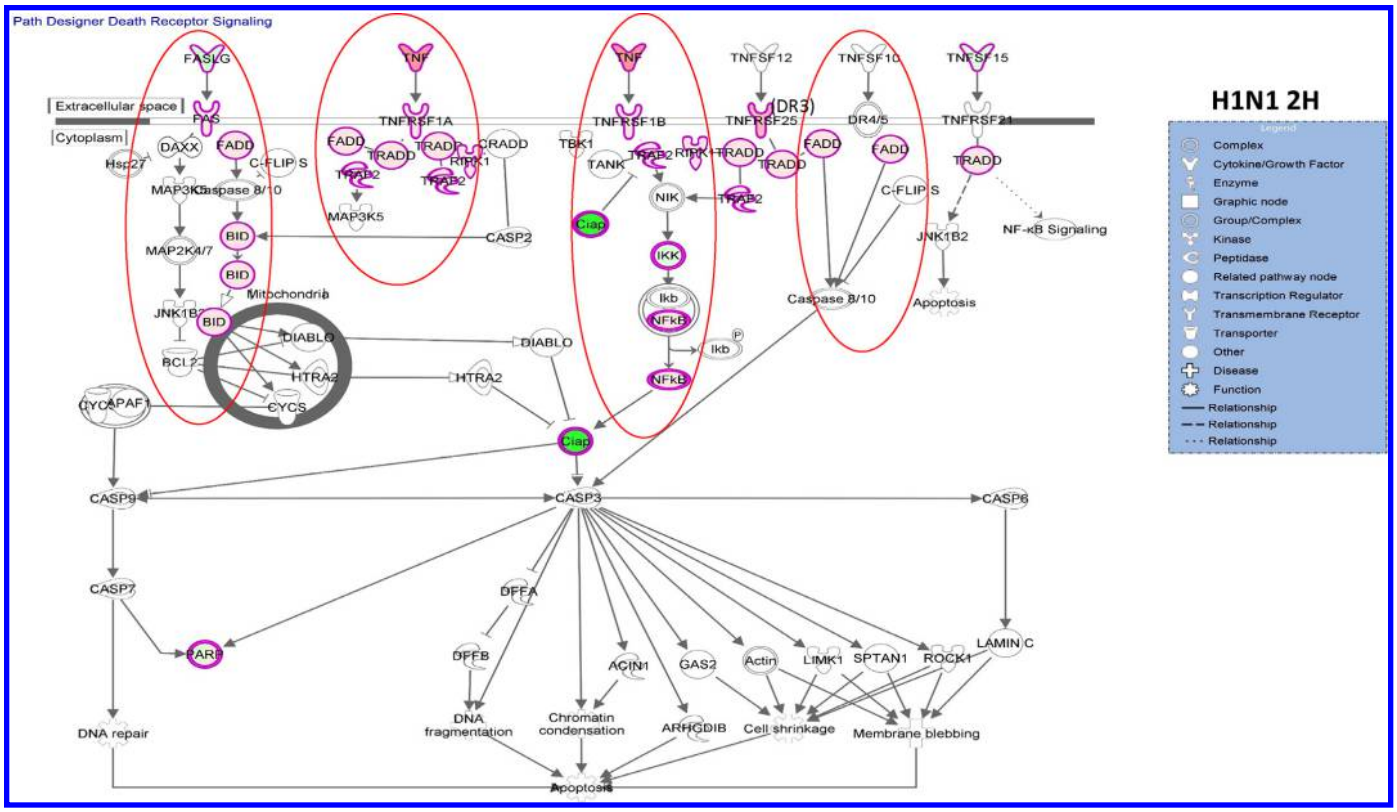


Fig. 5. Ingenuity Pathway Analysis (IPA) network map depicting the DR signaling changes in HBEpCs after 2 h of infection with IAV H1N1. Up- and downregulated genes in red and green, respectively. This figure shows the direct (solid lines) and indirect (dashed lines) interactions reported for the DR pathway genes. Biological network analysis was performed with IPA software and statistical significance with Fisher's exact test.

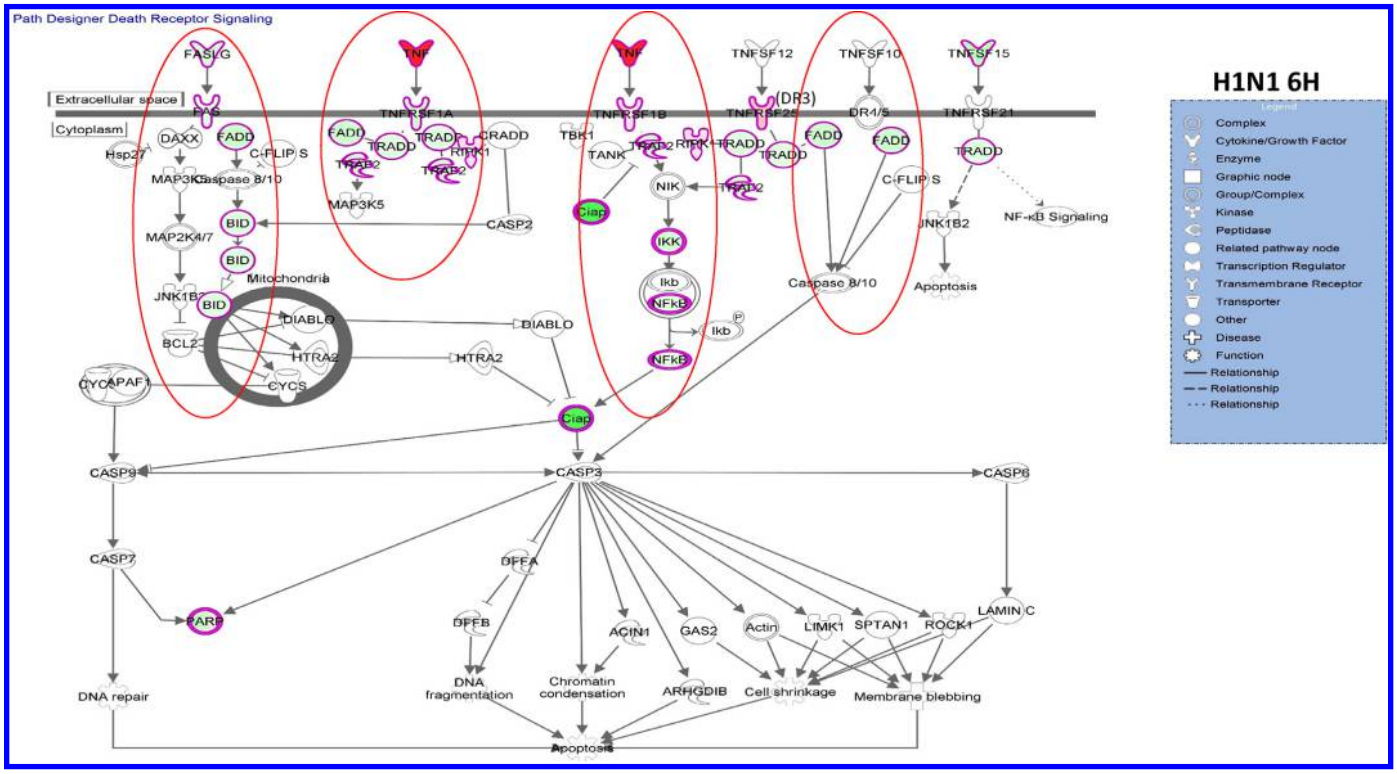


Fig. 6. IPA network map depicting the DR signaling changes in HBEpCs after 6 h of infection with IAV H1N1. Up- and downregulated genes in red and green, respectively. This figure shows the direct (solid lines) and indirect (dashed lines) interactions reported for the DR pathway genes. Biological network analysis was performed by using IPA software and statistical significance with Fisher's exact test.

FasR trimerization, followed by signaling through the adaptor protein FADD and the recruitment of caspase-8 (Fig. 5). As a result, caspase-8 undergoes oligomerization and subsequent activation via autocatalysis. Activated caspase-8 then stimulates apoptosis either by directly cleaving and activating the executioner caspase, caspase-3, or by cleaving BID. Previous studies have shown that tBID translocates to the mitochondria and induces cytochrome c release (12). Cytochrome c binds and activates apoptotic peptidase activating factor 1 (APAF-1) as well as caspase-9 (15). Activation of caspase-9 in turn cleaves downstream effector caspase-3. Our data (Fig. 5) suggest that influenza infection induces key factors of the DR pathway such as Fas, FADD, DR3, DR5, and both caspases-3 and -8. It has been reported that the activation of caspase-8 results in the cleavage of the BCL-2-family protein BID (1.6-fold increase, 2 h post-H1N1 infection). Increased host immune and death responses also has been reported in a mouse model exposed to the recombinant 1918 pandemic IAV (18). Moreover, results from our laboratory showed increased release of Cytochrome oxidase 6C (COX6C) 1–3 h postinfection in HBEpCs, which gradually decreased by 6 h exposure to IAV (25), and that apoptosis is initiated early following IAV infection of HeLa cells and A549 cells (26, 31).

Several viruses trigger apoptosis early in infection either when viruses interact with receptors on the cellular surface or at the time of fusion with the cell membrane and disassembly (4, 14). In contrast, certain viruses induce apoptosis at late stages of viral replication, providing a mechanism for dissemination of progeny virus. Several viral proteins were involved in the regulation of the mitochondrial apoptotic pathway (18). Following assembly and maturation inside the host cell, IAV may rely on apoptotic pathways as a mechanism to release progeny virus into the neighboring healthy cells. Apoptosis as an exit strategy from the host cells has been reported in other viruses such as Calciviruses (3, 30).

Caspase-8 is activated through multiple DR pathway genes. The DR3 promoted apoptosis through the adaptor proteins FADD. leading to the activation of caspase-8 (Fig. 4). Fas ligand binds to Fas and initiates the activation of FADD. Activated FADD in turn recruits caspase-8, which activates caspase-9 through BID. In the absence of caspase activation, initiation of DR pathway leads to the activation of an alternative programmed cell death pathway termed necroptosis. Recent studies with murine fibroblast and airway epithelial cells showed RIPK3-dependent necroptosis on exposure to IAV (23). Our data also showed a decrease in RIPK3 mRNA expression 6 h postinfection with IAV.

Receptor genes involved in the regulation of the apoptosis pathway in HBEpCs infected with IAV have a significant role in modulating cell survival. The level of FADD was increased in the first hour of exposure to IAV and by 3 h showed a gradual decline that reached a significant downregulation by 6 h (Fig. 1). The data suggest that the virus takes control (3–6 h post infection) of the translation machinery and modulates host gene expression. A similar observation was reported in HeLa and MDCK cells infected with IAV (31). Three caspases appear to be involved in apoptosis mediated by IAV infection: caspase-9 (25), and caspases-3 (36), and caspase-8. Caspase-3 and caspase-8 were decreased in their expression levels (2–6 h postinfection), allowing the HBEpCs to recover from apopto-

sis. We also observed a decrease in apoptotic cells after 6 h exposure to IAV when compared with exposure after 2 h. These data were in concordance with our previous report showing a decrease in phosphorylated caspases 9 (27). Studies in a mouse model infected with r1918 IAV reported significant induction of mRNAs for FAS, caspase-8, and caspase-9 (18).

From the PCR superarray data and the IPA, it is clear that 2 h post-IAV infection leads to the downregulation of several genes that inhibit viral survival in host cells. These genes include reactive oxygen species (ROS)-related genes NADPH oxidase 1 (NOX11) (6- to 7-fold downregulation) and NOX4 (1- to 3.5-fold downregulation) at 6 h post exposure of IAV (Table 1). The exact mechanism of how the virus downregulates these genes, however, is not clear. Necroptosis key protein MLKL is activated by phosphorylation and is mediated by RIP1. In our study, we observed a slight decrease in the levels of RIPK1 at 6 h (1.6-fold in both strains) compared with 2 h (1.9, H1N1; and 2.14, H3N2). The kinase domain of RIPK1 plays different roles in cell survival and is important in necroptosis induction (19).

In conclusion, IAV infection initially leads to reprogramming of host cell genes that ultimately drive these cells into an apoptotic state, but later in the infection process, these proapoptotic genes are downregulated to favor host cell survival and replication of the virus. Within the first 2 h of infection, the host cell may respond to the virus by entering into apoptosis to abrogate the virus from replicating. Nevertheless, thereafter, the virus can overcome the cells' defense response and force the cells to downregulate genes like those in the DR pathway. This report shows the significant role of the DR genes at an early stage (2 h) of IAV infection. Modulating the early-stage DR genes may be of use in immunotherapeutic intervention to block IAV replication. Understanding the contribution of host immune responses to IAV infection may lead to identification of biomarkers of infection and the development of novel antiviral therapies.

## DISCLAIMERS

The findings and conclusions in this study are those of the authors and do not necessarily represent the views of National Institute of Occupational Safety and Health, Centers for Disease Control and Prevention.

## DISCLOSURES

No conflicts of interest, financial or otherwise, are declared by the authors.

## AUTHOR CONTRIBUTIONS

S.O., D.H.B., and J.D.N. conceived and designed research; S.O. performed experiments; S.O. analyzed data; S.O., D.H.B., and J.D.N. interpreted results of experiments; S.O. prepared figures; S.O., D.H.B., and J.D.N. drafted manuscript; S.O., D.H.B., and J.D.N. edited and revised manuscript; S.O., D.H.B., and J.D.N. approved final version of manuscript.

## REFERENCES


1. The evolution of human influenza viruses. *Philos Trans R Soc Lond B Biol Sci* 356: 1861–1870, 2001. doi:10.1098/rstb.2001.0999.
2. **Aldridge JR Jr, Moseley CE, Boltz DA, Negovetich NJ, Reynolds C, Franks J, Brown SA, Doherty PC, Webster RG, Thomas PG.** TNF/iNOS-producing dendritic cells are the necessary evil of lethal influenza virus infection. *Proc Natl Acad Sci USA* 106: 5306–5311, 2009. doi:10.1073/pnas.0900655106.
3. **Alonso C, Oviedo JM, Martín-Alonso JM, Díaz E, Boga JA, Parra F.** Programmed cell death in the pathogenesis of rabbit hemorrhagic disease. *Arch Virol* 143: 321–332, 1998. doi:10.1007/s007050050289.
4. **Barton ES, Chappell JD, Connolly JL, Forrest JC, Dermody TS.** Reovirus receptors and apoptosis. *Virology* 290: 173–180, 2001. doi:10.1006/viro.2001.1160.
5. **Centers for Disease Control and Prevention.** Disease Burden of Influenza. https://www.cdc.gov/flu/about/disease/burden.htm 2017.
6. **Centers for Disease Control and Prevention.** Influenza (Flu) In the workplace. https://www.cdc.gov/niosh/topics/flu/activities.html 2017.
7. **Chinnaiyan AM, O'Rourke K, Tewari M, Dixit VM.** FADD, a novel death domain-containing protein, interacts with the death domain of Fas and initiates apoptosis. *Cell* 81: 505–512, 1995. doi:10.1016/0092-8674(95)90071-3.
8. **Czabotar PE, Lessene G, Strasser A, Adams JM.** Control of apoptosis by the BCL-2 protein family: implications for physiology and therapy. *Nat Rev Mol Cell Biol* 15: 49–63, 2014. doi:10.1038/nrm3722.
9. **Danial NN, Korsmeyer SJ.** Cell death: critical control points. *Cell* 116: 205–219, 2004. doi:10.1016/S0092-8674(04)00046-7.
10. **Duprez L, Wirawan E, Vanden Berghe T, Vandenabeele P.** Major cell death pathways at a glance. *Microbes Infect* 11: 1050–1062, 2009. doi:10.1016/j.micinf.2009.08.013.
11. **Elmore S.** Apoptosis: a review of programmed cell death. *Toxicol Pathol* 35: 495–516, 2007. doi:10.1080/01926230701320337.
12. **Epand RF, Martinou JC, Montessuit S, Epand RM, Yip CM.** Direct evidence for membrane pore formation by the apoptotic protein Bax. *Biochem Biophys Res Commun* 298: 744–749, 2002. doi:10.1016/S0006-291X(02)02544-5.
13. **Iwai A, Shiozaki T, Miyazaki T.** Relevance of signaling molecules for apoptosis induction on influenza A virus replication. *Biochem Biophys Res Commun* 441: 531–537, 2013. doi:10.1016/j.bbrc.2013.10.100.
14. **Jan JT, Chatterjee S, Griffin DE.** Sindbis virus entry into cells triggers apoptosis by activating sphingomyelinase, leading to the release of ceramide. *J Virol* 74: 6425–6432, 2000. doi:10.1128/JVI.74.14.6425-6432.2000.
15. **Jiang X, Wang X.** Cytochrome C-mediated apoptosis. *Annu Rev Biochem* 73: 87–106, 2004. doi:10.1146/annurev.biochem.73.011303.073706.
16. **Jiménez-Marín Á, Collado-Romero M, Ramirez-Boo M, Arce C, Garrido JJ.** Biological pathway analysis by ArrayUnlock and Ingenuity Pathway Analysis. *BMC Proc* 3, *Suppl* 4: S6, 2009. doi:10.1186/1753-6561-3-s4-s6.
17. **Karlas A, Machuy N, Shin Y, Pleissner KP, Artarini A, Heuer D, Becker D, Khalil H, Ogilvie LA, Hess S, Mäurer AP, Müller E, Wolff T, Rudel T, Meyer TF.** Genome-wide RNAi screen identifies human host factors crucial for influenza virus replication. *Nature* 463: 818–822, 2010. doi:10.1038/nature08760.
18. **Kash JC, Tumpey TM, Proll SC, Carter V, Perwitasari O, Thomas MJ, Basler CF, Palese P, Taubenberger JK, García-Sastre A, Swayne DE, Katze MG.** Genomic analysis of increased host immune and cell death responses induced by 1918 influenza virus. *Nature* 443: 578–581, 2006. doi:10.1038/nature05181.
19. **Liao Y, Wang HX, Mao X, Fang H, Wang H, Li Y, Sun Y, Meng C, Tan L, Song C, Qiu X, Ding C.** RIP1 is a central signaling protein in regulation of TNF-α/TRAIL mediated apoptosis and necroptosis during Newcastle disease virus infection. *Oncotarget* 8: 43201–43217, 2017. doi:10.18632/oncotarget.17970.
20. **Lin C, Zimmer SG, Lu Z, Holland RE Jr, Dong Q, Chambers TM.** The involvement of a stress-activated pathway in equine influenza virus-mediated apoptosis. *Virology* 287: 202–213, 2001. doi:10.1006/viro.2001.1010.
21. **Ludwig S, Pleschka S, Planz O, Wolff T.** Ringing the alarm bells: signalling and apoptosis in influenza virus infected cells. *Cell Microbiol* 8: 375–386, 2006. doi:10.1111/j.1462-5822.2005.00678.x.
22. **Miyazaki T, Reed JC.** A GTP-binding adapter protein couples TRAIL receptors to apoptosis-inducing proteins. *Nat Immunol* 2: 493–500, 2001. doi:10.1038/88684.
23. **Nogusa S, Thapa RJ, Dillon CP, Liedmann S, Oguin TH III, Ingram JP, Rodriguez DA, Kosoff R, Sharma S, Sturm O, Verbist K, Gough PJ, Bertin J, Hartmann BM, Sealfon SC, Kaiser WJ, Mocarski ES, López CB, Thomas PG, Oberst A, Green DR, Balachandran S.** RIPK3 Activates Parallel Pathways of MLKL-Driven Necroptosis and FADD-Mediated Apoptosis to Protect against Influenza A Virus. *Cell Host Microbe* 20: 13–24, 2016. doi:10.1016/j.chom.2016.05.011.
24. **Othumpangat S, Gibson LF, Samsell L, Piedimonte G.** NGF is an essential survival factor for bronchial epithelial cells during respiratory syncytial virus infection. *PLoS One* 4: e6444, 2009. doi:10.1371/journal.pone.0006444.

25. **Othumpangat S, Noti JD, Beezhold DH.** Lung epithelial cells resist influenza A infection by inducing the expression of cytochrome c oxidase VIc which is modulated by miRNA 4276. *Virology* 468–470: 256–264, 2014. doi:10.1016/j.virol.2014.08.007.
26. **Othumpangat S, Noti JD, Blachere FM, Beezhold DH.** Expression of non-structural-1A binding protein in lung epithelial cells is modulated by miRNA-548an on exposure to influenza A virus. *Virology* 447: 84–94, 2013. doi:10.1016/j.virol.2013.08.031.
27. **Othumpangat S, Noti JD, McMillen CM, Beezhold DH.** ICAM-1 regulates the survival of influenza virus in lung epithelial cells during the early stages of infection. *Virology* 487: 85–94, 2016. doi:10.1016/j.virol.2015.10.005.
28. **Ray SD, Corcoran GB.** Apoptosis and cell death, in *General and Applied Toxicology* (Ballantyne B, Marrs T, Syversion T, editors). Chichester, UK: John Wiley & Sons, 2009, p. 247–312.
29. **Schultz-Cherry S, Dybdahl-Sissoko N, Neumann G, Kawaoka Y, Hinshaw VS.** Influenza virus ns1 protein induces apoptosis in cultured cells. *J Virol* 75: 7875–7881, 2001. doi:10.1128/JVI.75.17.7875-7881.2001.
30. **Sosnovtsev SV, Prikhod'ko EA, Belliot G, Cohen JI, Green KY.** Feline calicivirus replication induces apoptosis in cultured cells. *Virus Res* 94: 1–10, 2003. doi:10.1016/S0168-1702(03)00115-1.
31. **Takizawa T, Matsukawa S, Higuchi Y, Nakamura S, Nakanishi Y, Fukuda R.** Induction of programmed cell death (apoptosis) by influenza virus infection in tissue culture cells. *J Gen Virol* 74: 2347–2355, 1993. doi:10.1099/0022-1317-74-11-2347.
32. **Taubenberger JK, Morens DM.** The pathology of influenza virus infections. *Annu Rev Pathol* 3: 499–522, 2008. doi:10.1146/annurev.pathmechdis.3.121806.154316.
33. **Tumpey TM, Lu X, Morken T, Zaki SR, Katz JM.** Depletion of lymphocytes and diminished cytokine production in mice infected with a highly virulent influenza A (H5N1) virus isolated from humans. *J Virol* 74: 6105–6116, 2000. doi:10.1128/JVI.74.13.6105-6116.2000.
34. **Wang X, Tan J, Zoueva O, Zhao J, Ye Z, Hewlett I.** Novel pandemic influenza A (H1N1) virus infection modulates apoptotic pathways that impact its replication in A549 cells. *Microbes Infect* 16: 178–186, 2014. doi:10.1016/j.micinf.2013.11.003.
35. **Wurzer WJ, Ehrhardt C, Pleschka S, Berberich-Siebelt F, Wolff T, Walczak H, Planz O, Ludwig S.** NF-kappaB-dependent induction of tumor necrosis factor-related apoptosis-inducing ligand (TRAIL) and Fas/FasL is crucial for efficient influenza virus propagation. *J Biol Chem* 279: 30931–30937, 2004. doi:10.1074/jbc.M403258200.
36. **Wurzer WJ, Planz O, Ehrhardt C, Giner M, Silberzahn T, Pleschka S, Ludwig S.** Caspase 3 activation is essential for efficient influenza virus propagation. *EMBO J* 22: 2717–2728, 2003. doi:10.1093/emboj/cdg279.
37. **Yatim N, Albert ML.** Dying to replicate: the orchestration of the viral life cycle, cell death pathways, and immunity. *Immunity* 35: 478–490, 2011. doi:10.1016/j.immuni.2011.10.010.
38. **Zhou X, Jiang W, Liu Z, Liu S, Liang X.** Virus Infection and Death Receptor-Mediated Apoptosis. *Viruses* 9: E316, 2017. doi:10.3390/v9110316.